

Unconventional photon blockade under the combined effects of optical parametric amplification and two-photon dissipation

Li Yan(闫丽), Ling-Juan Feng(封玲娟), Rui Cao(曹瑞)

Citation: Chin. Phys. B. 35, 090308 (2026). DOI: 10.1088/1674-1056/ae9fbf | CSTR: 32038.14.CPB.ae9fbf
http://cpb.iphy.ac.cn; http://iopscience.iop.org/cpb

What follows is a list of articles you may be interested in

Robust quantum-like state simulation using k-regular bipartite networks

Xinjiang Zhou(周新疆), Tinggui Zhang(张廷桂)
Chin. Phys. B. 35, 090306 (2026). DOI: 10.1088/1674-1056/ae5c75 | CSTR: 32038.14.CPB.ae5c75

Bipartite and tripartite entanglement in the two-qubit quantum Rabi model

Lijun Mao(毛丽君), Hongmei Wang(王红梅), Yaoyao Zhou(周瑶瑶), Hui Guo(郭慧)
Chin. Phys. B. 35, 080303 (2026). DOI: 10.1088/1674-1056/ae85f7 | CSTR: 32038.14.CPB.ae85f7

Hierarchy of average correlation, quantum steering and Bell nonlocality in two-qubit systems

Qinglong Tian(田清龙), Youneng Guo(郭有能)
Chin. Phys. B. 35, 080302 (2026). DOI: 10.1088/1674-1056/ae6b38 | CSTR: 32038.14.CPB.ae6b38

Unconventional photon blockade in the two-photon Jaynes–Cummings model with two-frequency cavity drivings and atom driving

Xin Liu(刘欣), Meng-Yu Tian(田梦雨), Xiao-Ning Cui(崔晓宁), Xin-He Zhang(张馨鹤)
Chin. Phys. B. 33, 020308 (2024). DOI: 10.1088/1674-1056/ad0cca

Unconventional photon blockade in a three-mode system with double second-order nonlinear coupling

Hong-Yu Lin(林宏宇), Hui Yang(杨慧), Zhi-Hai Yao(姚治海)
Chin. Phys. B. 29, 120304 (2020). DOI: 10.1088/1674-1056/abab82

Unconventional photon blockade under the combined effects of optical parametric amplification and two-photon dissipation

Li Yan(闫丽)[1], Ling-Juan Feng(封玲娟)[2,†], and Rui Cao(曹瑞)[3,‡]

[1] *College of Physics and Electronic Engineering, Heze University, Heze* 274015, *China*
[2] *School of Sciences, Shanghai Institute of Technology, Shanghai* 201418, *China*
[3] *School of Mathematics and Statistics, Heze University, Heze* 274015, *China*

(Received 18 April 2026; revised manuscript received 10 July 2026; accepted manuscript online 28 August 2026)

Unconventional photon blockade (UPB) is an important quantum phenomenon that relies on the quantum interference effect. Here, we propose coupling an optical parametric amplifier (OPA) to a Kerr nonlinear single-mode cavity in a two-photon dissipation environment, enabling strong photon antibunching based on the UPB mechanism. The optimal conditions for achieving UPB are first derived analytically. The results are subsequently compared with the second-order correlation function derived from numerical simulations, and excellent agreement is observed. The findings show that UPB is enhanced without significantly reducing the mean photon number. This further demonstrates that the width of the UPB occurrence window increases with increasing OPA coefficient and driving laser intensity. Finally, theoretical analysis reveals the physical mechanism of UPB, showing that the Kerr medium is not the dominant factor for UPB generation in this system. Thus, our work offers valuable theoretical guidance for precisely controlling UPB and optimizing single-photon source performance.

Keywords: unconventional photon blockade, two-photon dissipation, optical parametric amplifier

PACS: 03.67.–a, 42.50.–p, 42.50.Dv

DOI: 10.1088/1674-1056/ae9fbf **CSTR:** 32038.14.CPB.ae9fbf

1. Introduction

The generation and manipulation of single-photon sources[1–3] have significant applications in quantum simulation,[4,5] quantum metrology,[6,7] and quantum information and communication technologies.[8,9] Photon blockade (PB),[10–13] an effective method for obtaining such sources, has attracted extensive attention in recent decades. PB can be realized through two distinct physical mechanisms. One is conventional photon blockade (CPB),[14–17] arising from the anharmonic eigenenergy of the system, which requires a strong nonlinearity (atom-cavity coupling or a Kerr nonlinearity of the cavity). For CPB, the resonance excitation of a single photon suppresses the simultaneous excitation of a second photon. The single-photon source generated by CPB has a large mean photon number, corresponding to high brightness but poor purity. The other, unconventional photon blockade (UPB),[18–22] by contrast, originates from destructive interference among multiple two-photon excitation channels. Although it has relatively low requirements for nonlinearity, it still needs at least one additional component, such as an auxiliary cavity, an atom or an auxiliary driving field, to construct two or more excitation paths together with the original system. For UPB, when the system parameters meet the optimal conditions, it completely suppresses the two-photon excitation. However, the brightness is limited by the design of the auxiliary mode.

Therefore, it remains a challenge to enhance the purity of single-photon sources while maintaining high brightness. Recently, several articles have studied PB induced by two-photon dissipation.[23–27] In particular, Ref. [23] showed that environmentally induced PB (EPB) generated solely by two-photon dissipation can achieve a large single-photon occupancy under weak driving conditions, exhibiting higher brightness than that of CPB. Feng *et al.*[24] extended EPB to cavity quantum electrodynamics (QED) and demonstrated that even with weak coupling, a strong antibunching effect can be generated when the cavity resonates with the atom. Inspired by the above-mentioned works, we explore UPB assisted by an optical parametric amplifier (OPA) in a two-photon dissipation environment. The theoretical and numerical results show that introducing the two-photon dissipation at resonance enhances UPB and yields a larger average number of photons. In contrast to the conventional UPB, the UPB in this work is enhanced by combining it with two-photon dissipation, broadening the occurrence window while maintaining high brightness. It is worth noting that our proposal differs from Ref. [25] as follows: Firstly, our model incorporates both two-photon and single-photon dissipative processes, the latter having been neglected in previous studies. Secondly, we replace the two coupled cavities of Ref. [26] with a single-mode cavity, introduc-

†Corresponding author. E-mail: lingjuanfeng@sit.edu.cn
‡Corresponding author. E-mail: ruicao999@126.com

© 2026 Chinese Physical Society and IOP Publishing Ltd. All rights, including for text and data mining, AI training, and similar technologies, are reserved.

ing an OPA to construct the interference pathway.

Our work is structured as follows. In Section 2, we present the system model and introduce the master equation that incorporates both two-photon and single-photon dissipative processes. We also adopt an effective non-Hermitian Hamiltonian to describe the single-photon loss. Within this framework, we derive the optimal conditions for UPB by solving the effective non-Hermitian dynamics, and obtain the second-order correlation function and the mean photon number to characterize the photon statistics. In Section 3, we verify the optimal conditions by numerical simulations and investigate the effect of two-photon dissipation on UPB. In Section 4, we further discuss the effects of other system parameters (driving strength Ω, the nonlinear gain G of the optical parametric amplifier, and driving phase ϕ) on UPB in detail. Finally, we summarize our main findings and conclude in Section 5.

2. Theoretical model

We consider a quantum hybrid system, which consists of a degenerate optical parametric amplifier (OPA) and a single-mode cavity with a Kerr medium. We assume that the single-mode cavity is driven by a laser field at frequency ω_l with strength Ω. In a frame rotating at the laser frequency, the Hamiltonian of this system can be expressed as

$$\begin{aligned} H_1 &= \Delta a^\dagger a + U a^\dagger a^\dagger a a + \mathrm{i}G\left(a^{\dagger 2} - a^2\right) \\ &\quad + \Omega\left(a^\dagger \mathrm{e}^{\mathrm{i}\phi} + a\mathrm{e}^{-\mathrm{i}\phi}\right), \end{aligned} \tag{1}$$

where a^+ (a) is the creation (annihilation) operator of the single-mode cavity with the frequency ω_a, $\Delta = \omega_a - \omega_l$ is the detuning of the single-mode cavity from the laser drive, G is the nonlinear coefficient of the OPA, U is the Kerr nonlinearity strength, and ϕ is the phase of the driving laser.

In addition to the cavity driving and OPA in the considered system, the optical dissipations (i.e., one- and two-photon losses) are usually appreciable and cannot be ignored.[28,29] Thus, we describe these dissipations in terms of the following master equation for the density matrix ρ:

$$\begin{aligned} \frac{\mathrm{d}\hat{\rho}}{\mathrm{d}t} &= -\mathrm{i}\left[\hat{H}_1, \hat{\rho}\right] + \kappa\left(\hat{a}\hat{\rho}\hat{a}^\dagger - \frac{1}{2}\hat{a}^\dagger\hat{a}\hat{\rho} - \frac{1}{2}\hat{\rho}\hat{a}^\dagger\hat{a}\right) \\ &\quad + \kappa_2\left(\hat{a}\hat{a}\hat{\rho}\hat{a}^\dagger\hat{a}^\dagger - \frac{1}{2}\hat{a}^\dagger\hat{a}^\dagger\hat{a}\hat{a}\hat{\rho} - \frac{1}{2}\hat{\rho}\hat{a}^\dagger\hat{a}^\dagger\hat{a}\hat{a}\right), \end{aligned} \tag{2}$$

where the parameters κ and κ_2 represent the one- and two-photon dissipation rates, respectively.

Since we only consider the steady-state solution ρ_s, the average photon number and the equal-time second-order correlation function are defined as

$$\langle n\rangle = \left\langle a^\dagger a\right\rangle = \mathrm{Tr}(\rho_s a^\dagger a), \tag{3}$$

$$g^{(2)}(0) = \frac{\left\langle a^{\dagger 2}a^2\right\rangle}{\left\langle a^\dagger a\right\rangle^2} = \frac{\mathrm{Tr}\left(\rho_s a^{\dagger 2}a^2\right)}{\left[\mathrm{Tr}\left(\rho_s a^\dagger a\right)\right]^2}. \tag{4}$$

Here, the value of $g^{(2)}(0)$ characterizes the probability of detecting two photons at the same time. The condition $g^{(2)}(0) > 1$ manifests as super-Poissonian statistics (photon bunching effect), while $g^{(2)}(0) < 1$ corresponds to sub-Poissonian statistics, referring to photon antibunching. When $g^{(2)}(0) \to 0$, a complete photon blockade (PB) occurs in the cavity, which implies that two photons are never detected simultaneously.

In the following, we calculate $g^{(2)}(0)$ and $\langle n\rangle$ analytically, and then derive the optimal conditions for UPB. Based on the weak-driving assumption, i.e., $\Omega \ll \kappa$, we truncate the system to states with at most two photons. In the non-Hermitian Hamiltonian approach, the steady-state density matrix is approximated by a pure state $|\psi\rangle$,

$$|\psi\rangle = C_0|0\rangle + C_1|1\rangle + C_2|2\rangle, \tag{5}$$

where $|n\rangle$ denotes the photon number Fock-state basis, and C_n is the probability amplitude of the corresponding basis state $|n\rangle$.

By employing the quantum-jump method of Ref. [30] and phenomenologically incorporating two-photon dissipation,[31–33] we obtain the effective non-Hermitian Hamiltonian

$$\begin{aligned} H' &= \Delta a^\dagger a + U a^\dagger a^\dagger a a + \mathrm{i}G\left(a^{\dagger 2} - a^2\right) \\ &\quad + \Omega\left(a^\dagger \mathrm{e}^{\mathrm{i}\phi} + a\mathrm{e}^{-\mathrm{i}\phi}\right) - \mathrm{i}\frac{\kappa}{2}a^\dagger a - \mathrm{i}\frac{\kappa_2}{2}a^\dagger a^\dagger a a. \end{aligned} \tag{6}$$

In fact, the quantum-jump term can be ignored under weak driving, and the effective Hamiltonian can be derived from the master equation (2).[25,34] To demonstrate that the non-Hermitian Hamiltonian approach provides a valid approximation to the two-photon dissipation master equation, we employ the non-Hermitian Hamiltonian to derive analytical solutions for $g^{(2)}(0)$ and $\langle n\rangle$ under the optimal condition for UPB in Section 3. These analytical results show excellent agreement with the corresponding quantities obtained from the numerical steady state of the full master equation (see Fig. 2).

Substituting the state (5) and the non-Hermitian Hamiltonian (6) into the Schrödinger equation $\mathrm{i}\frac{\mathrm{d}|\psi\rangle}{\mathrm{d}t} = H'|\psi\rangle$, we obtain a set of equations for the coefficients

$$\begin{aligned} \mathrm{i}\dot{C}_0 &= \Omega\,\mathrm{e}^{-\mathrm{i}\phi}C_1 - \mathrm{i}\sqrt{2}GC_2, \\ \mathrm{i}\dot{C}_1 &= \Omega\,\mathrm{e}^{\mathrm{i}\phi}C_0 + \left(\Delta - \mathrm{i}\frac{\kappa}{2}\right)C_1 + \sqrt{2}\Omega\,\mathrm{e}^{-\mathrm{i}\phi}C_2, \\ \mathrm{i}\dot{C}_2 &= \mathrm{i}\sqrt{2}GC_0 + \sqrt{2}\Omega\,\mathrm{e}^{\mathrm{i}\phi}C_1 \\ &\quad + (2\Delta - \mathrm{i}\kappa - \mathrm{i}\kappa_2 + 2U)C_2. \end{aligned} \tag{7}$$

With the steady-state assumption, we obtain the coefficients by solving the following coupled equations:

$$\begin{aligned} 0 &= \Omega\,\mathrm{e}^{-\mathrm{i}\phi}C_1 - \mathrm{i}\sqrt{2}GC_2, \\ 0 &= \Omega\,\mathrm{e}^{\mathrm{i}\phi}C_0 + \left(\Delta - \mathrm{i}\frac{\kappa}{2}\right)C_1 + \sqrt{2}\Omega\,\mathrm{e}^{-\mathrm{i}\phi}C_2, \\ 0 &= \mathrm{i}\sqrt{2}GC_0 + \sqrt{2}\Omega\,\mathrm{e}^{\mathrm{i}\phi}C_1 \end{aligned}$$

$$+(2\Delta-\mathrm{i}\kappa-\mathrm{i}\kappa_2+2U)C_2. \tag{8}$$

Under the weak-driving condition with $C_0 \gg C_1 \gg C_2$, we assume $C_0 \approx 1$ for the convenience of calculation. By neglecting the higher-order terms, we have the approximate analytical solutions for the amplitudes

$$C_1 = -\frac{2\Omega\,\mathrm{e}^{\mathrm{i}\phi}}{2\Delta-\mathrm{i}\kappa}, \tag{9}$$

$$C_2 = \frac{\sqrt{2}\left(2\mathrm{e}^{2\mathrm{i}\phi}\Omega^2-2\mathrm{i}G\Delta-G\kappa\right)}{(2\Delta-\mathrm{i}\kappa)\,(2U+2\Delta-\mathrm{i}\kappa-\mathrm{i}\kappa_2)}. \tag{10}$$

Using the previous definitions and combining Eqs. (3)–(5), $g^{(2)}(0)$ and $\langle n\rangle$ in the steady state are approximated as

$$g^{(2)}(0) = \frac{2\,|C_2|^2}{\left(|C_1|^2+2\,|C_2|^2\right)^2} \approx \frac{2\,|C_2|^2}{|C_1|^4}, \tag{11}$$

and

$$\langle n\rangle = |C_1|^2+2\,|C_2|^2 \approx |C_1|^2. \tag{12}$$

According to the expression for $g^{(2)}(0)$ above, if $C_2=0$, we have $g^{(2)}(0)=0$, that is,

$$2\mathrm{e}^{2\mathrm{i}\phi}\Omega^2-2\mathrm{i}G\Delta-G\kappa=0. \tag{13}$$

UPB can be realized by setting the real and imaginary parts of Eq. (13) equal to zero. The optimal conditions are obtained as

$$G=\frac{2\Omega^2\cos 2\phi}{\kappa}, \quad \Delta=\frac{1}{2}\kappa\tan 2\phi. \tag{14}$$

Combining Eqs. (9)–(12), the steady-state solutions of the correlation function and the mean photon number become

$$g^{(2)}(0) = \frac{\left(4\Delta^2+\kappa^2\right)\left(2\Omega^2\mathrm{e}^{2\mathrm{i}\phi}-2\mathrm{i}G\Delta-G\kappa\right)\left(2\Omega^2\mathrm{e}^{-2\mathrm{i}\phi}+2\mathrm{i}G\Delta-G\kappa\right)}{4\Omega^4\left[4(U+\Delta)^2+(\kappa+\kappa_2)^2\right]}, \tag{15}$$

$$\langle n\rangle = \frac{4\Omega^2}{4\Delta^2+\kappa^2}. \tag{16}$$

We plot a full $g^{(2)}(0)$ map versus the parametric nonlinear coefficient and the detuning in Fig. 1. We can observe a deep blue region where $g^{(2)}(0)\ll 1$, which implies that photon blockade exists under appropriate parameter conditions. The red dashed line in the figure represents the result of Eq. (14), indicating the optimal condition for UPB. It can be seen that the optimal condition corresponds to the deep blue regime in which UPB is realized.

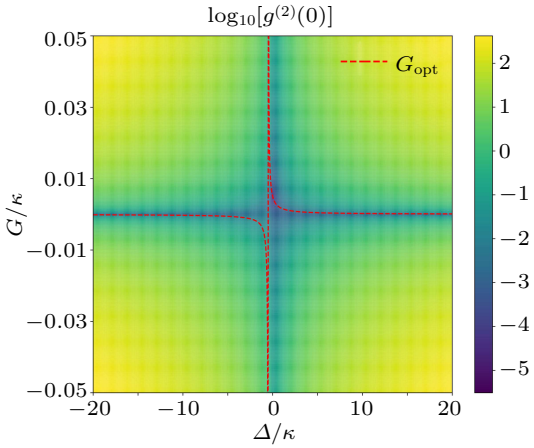


Fig. 1. The correlation function $g^{(2)}(0)$ with the nonlinear coefficient G/κ and Δ/κ, where $\Omega=0.05\kappa, U=0.5\kappa, \phi/\pi=0, \kappa_2=0$.

3. Effect of two-photon dissipation on UPB

In this section, the effect of two-photon dissipation on UPB will be discussed. For convenience, we uniformly adopt the single-photon decay rate κ as the reference unit. When the system parameters are set as $\Omega=0.05\kappa$, $U=0.5\kappa$, $\phi/\pi=0$, we get one set of optimal parameters from Eq. (14) $G_{\mathrm{opt}}=0.005\kappa$, $\Delta_{\mathrm{opt}}=0$. In Fig. 2(a), we plot the second-order correlation function $g^{(2)}(0)$ as a function of detuning Δ/κ with or without two-photon dissipation. The circles and the solid lines represent the numerical solutions based on Eqs. (1) and (2) and the analytical solutions based on Eq. (15), respectively. We find that, except for the minimal value of $g^{(2)}(0)$, a close match is observed between the numerical and analytical results. This difference is attributed to the truncation of the Hilbert space to two-photon excitation during the analytical solution process. In the resonant case ($\Delta=\omega_a-\omega_l=0$), the system will generate perfect photon blockade. In addition, the value of $g^{(2)}(0)$ is smaller in the presence of two-photon dissipation, i.e., the photon blockade effect is enhanced. This indicates that the single-photon source generated by UPB has higher purity. In addition, we note that when parameters deviate from the optimal values, i.e., Eq. (14) is not satisfied, the destructive quantum interference breaks down. Their superposition instead yields a substantial number of two-photon population, corresponding to an enhanced two-photon probability $|C_2|^2$. Since $g^{(2)}(0)\propto|C_2|^2$, this results in $g^{(2)}(0)>1$. Although two-photon dissipation is present, it merely consumes already-generated two-photon states without being able to restore the disrupted quantum interference; consequently, $g^{(2)}(0)$ remains greater than 1.

Figure 2(b) shows the effect of detuning on the mean photon number $\langle n\rangle$, and the result indicates that the peak of $\langle n\rangle$ corresponds to the valley of $g^{(2)}(0)$ at $\Delta = 0$. Furthermore, we compare the mean photon number versus detuning with and without two-photon dissipation. It is found that $\kappa_2 = 0$ (solid line) and $\kappa_2 = 10\kappa$ (dashed line) coincide. According to Eqs. (9) and (12), the mean photon number approximates the one-photon probability $|C_1|^2$ under weak driving. We observe that numerical and analytical results agree well, indicating that the system retains sufficient brightness despite two-photon dissipation. This work provides a reference for obtaining single-photon sources with high purity and brightness at resonance.

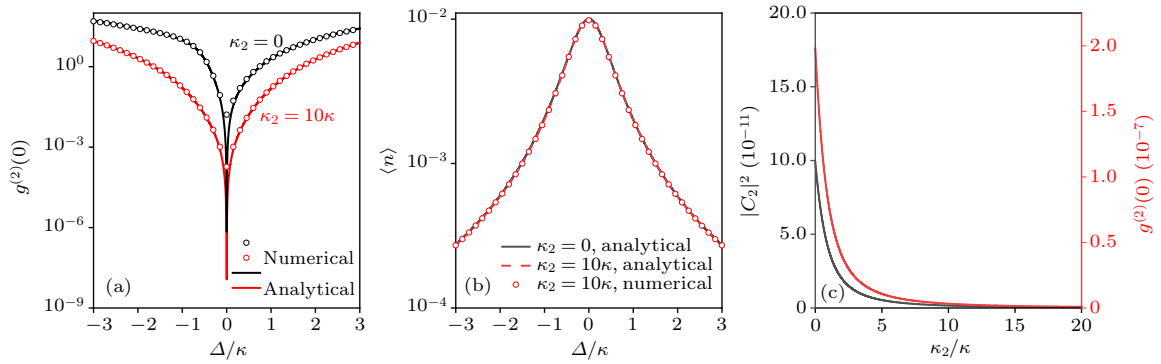


Fig. 2. (a) The correlation function $g^{(2)}(0)$ versus detuning Δ/κ under different two-photon decay rates κ_2 with $G_{\rm opt} = 0.005\kappa$, $\Delta_{\rm opt} = 0$. The solid curves correspond to the analytical solution from Eq. (15), while the circles describe the numerical result based on the master equation (2). (b) The mean photon number $\langle n\rangle$ versus detuning Δ/κ. (c) The correlation function $g^{(2)}(0)$ (red curve) given in Eq. (15) and the two-photon probability $|C_2|^2$ (black curve) given by Eq. (10) versus the two-photon decay rate. Other parameters are $\Omega = 0.05\kappa$, $U = 0.5\kappa$, $\phi/\pi = 0$.

Furthermore, to explore the effect of two-photon dissipation on UPB, we plot the two-photon probability $|C_2|^2$ and the correlation function $g^{(2)}(0)$ as a function of the two-photon decay rate κ_2 in Fig. 2(c). Clearly, as the two-photon decay rate increases, the two-photon probability $|C_2|^2$ drops significantly, thereby enhancing the UPB effect ($g^{(2)}(0) \to 0$), which can be explained by the analytical solutions based on Eqs. (10), (11), and (15). Therefore, two-photon dissipation is the key to reducing the two-photon probability. From a physics perspective, once two photons appear within the cavity, they simultaneously leak out (see Fig. 3).

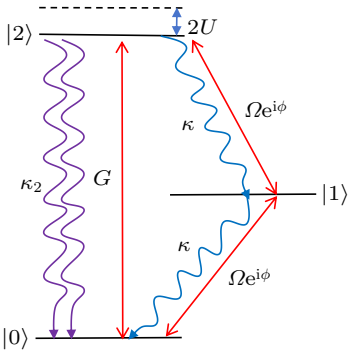


Fig. 3. Schematic diagram of system photon state transition pathways.

4. Effect of system parameters on UPB

From the optimal condition Eq. (14) in the previous text, we find that, apart from the cavity-laser detuning, other parameters also affect the occurrence of UPB. We then examine the effects of driving strength Ω, the OPA nonlinear coefficient G, and driving phase ϕ on the photon blockade phenomenon.

We first examine the dependence of the second-order correlation function on the OPA nonlinear coefficient G for various driving strengths. Figure 4 compares numerical results with analytical results: the solid curves are analytical solutions from Eq. (15), while circles correspond to numerical solutions from Eq. (2). Here, we set $\Delta = 0, \kappa_2 = 10\kappa$, and the other parameters are the same as those in Fig. 2. When $\Omega = 0.02\kappa, 0.04\kappa$, and 0.06κ, numerical and analytical results agree well except for the minima, for the same reason as in Fig. 2(a). Moreover, a stronger driving strength broadens the photon blockade window, thereby facilitating experimental observation of UPB and its applications.

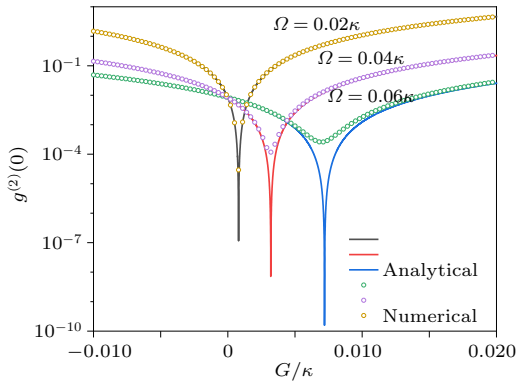


Fig. 4. The correlation function $g^{(2)}(0)$ with the nonlinear coefficient G/κ of the optical parametric amplifier under different driving strengths Ω/κ.

Then Fig. 5 plots the correlation function $g^{(2)}(0)$ versus the driving strength Ω for different nonlinear coefficients G. Similarly, the validity of the analytical approach is once again confirmed by the numerical simulations, as shown by the solid curves (analytical results) and the circles (numerical results).

The parameters are the same as those in Fig. 3. When the OPA nonlinear coefficient and driving strength satisfy the optimal condition in Eq. (14), perfect UPB is achieved. Moreover, the photon blockade window widens with increasing nonlinear coefficient. Thus, the results shown in Figs. 4 and 5 both indicate that choosing an appropriate driving strength and the OPA nonlinear coefficient facilitates photon blockade within a wider range.

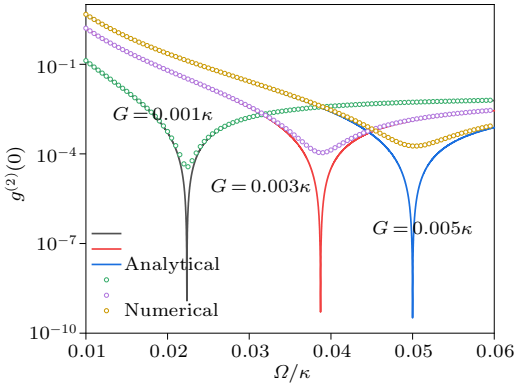


Fig. 5. The correlation function $g^{(2)}(0)$ with the driving strength Ω/κ under different nonlinear coefficients G/κ of the optical parametric amplifier.

To further investigate photon antibunching, we plot the variation of $g^{(2)}(0)$ with the phase ϕ in Fig. 6. As shown, the correlation function $g^{(2)}(0)$ exhibits periodic modulation by the driving phase with a period of π, reaching its minimum at $\phi = \pm\pi/2$, where the optimal condition $G_{\text{opt}} = -0.005\kappa$ can also be derived from Eq. (14). Under these conditions, a strong UPB effect emerges in the system. We utilize the relationship that the nonlinear coefficient is proportional to the cosine of the driving phase, demonstrating that the optimal nonlinear coefficient for perfect UPB remains unchanged, but the optimal driving phase varies.

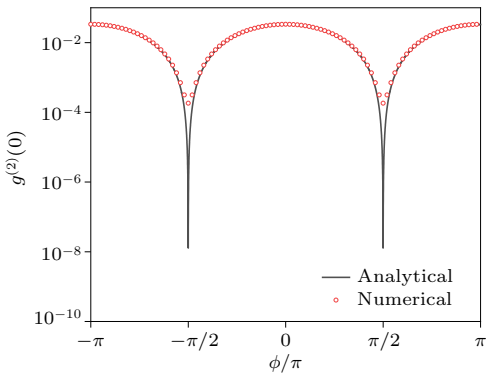


Fig. 6. The correlation function $g^{(2)}(0)$ versus driving phase with $\Omega = 0.05\kappa$; the parameters are the same as those in Fig. 4.

To explore the effect of Kerr nonlinearity on the photon blockade, we plot the correlation function $g^{(2)}(0)$ versus detuning for different Kerr nonlinearity strengths in Fig. 7. It is found that the absence of Kerr nonlinearity (solid line) yields behavior nearly identical to that with weak Kerr nonlinearity (dashed line), while $g^{(2)}(0)$ decreases slightly with increasing Kerr nonlinearity (dotted line). Notably, significant photon blockade persists regardless of whether Kerr nonlinearity is strong, weak, or absent. The underlying physical mechanism is illustrated in Fig. 3, which involves two paths reaching the two-photon state: the direct transition $|0\rangle \xrightarrow{G} |2\rangle$ is coupled by the optical parametric amplifier, while the indirect transition $|0\rangle \xrightarrow{\Omega e^{i\phi}} |1\rangle \xrightarrow{\Omega e^{i\phi}} |2\rangle$ proceeds sequentially from the ground state to the two-photon state via single-photon excitation by the driving laser field. Under the optimal condition of Eq. (14), destructive quantum interference between the two transition pathways eliminates two-photon excitation, thereby enabling strong photon blockade. The energy-level spacing can be tuned by Kerr nonlinearity, yet the interference between the photon transition pathways remains insensitive to it. This insensitivity ensures robust photon blockade across a wide range of Kerr nonlinearity strengths.

In Ref. [23], the authors compared EPB and CPB, and found that although EPB achieves a larger average photon number $\langle n\rangle$, CPB yields a smaller $g^{(2)}(0)$ due to the strong Kerr nonlinearity employed. By contrast, in our model, the synergistic effect of the Kerr nonlinearity and two-photon dissipation enables $g^{(2)}(0) \sim 10^{-8}$ when the parameters satisfy the optimal conditions, while maintaining a relatively high average photon number. Our scheme simultaneously improves the purity and maintains the brightness of the single-photon source. In Ref. [24], strong antibunching at resonance was demonstrated in cavity QED under weak coupling conditions through the introduction of two-photon dissipation; nevertheless, the mean photon number under weak driving remained substantially lower than that achieved in our system. Reference [25] reported a large mean photon number in a two-cavity coupled system based on two-photon dissipation; however, the resulting $g^{(2)}(0)$ was relatively high, which degrades the purity of the single-photon source.

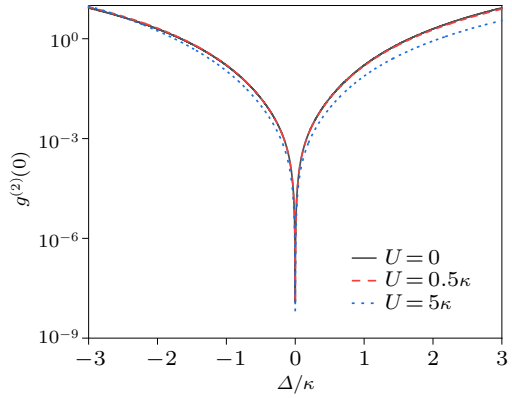


Fig. 7. The correlation function $g^{(2)}(0)$ versus detuning Δ/κ under different Kerr nonlinearity strengths with $G_{\text{opt}} = 0.005\kappa$, $\Delta_{\text{opt}} = 0$, the parameters are the same as those in Fig. 4.

Table 1. Comparison of this system with those in Refs. [23–25].

	Mechanism	$g^{(2)}(0)$	n	Operating parameters
This system	UPB + Kerr + two-photon dissipation	1.2×10^{-8}	0.01	$\Omega=0.05\kappa$, $U=0.5\kappa$, $G=0.005\kappa$, $\kappa_2=10\kappa$,
[23]	EPB/CPB	$0.003/8\times10^{-6}$	0.5/0.0016	$\Omega=0.02\kappa_2$, $U=10\kappa_2$, $\Delta=0$
[24]	EPB	0.045	6.4×10^{-7}	$\Omega=0.01\kappa$, $\kappa_2=10\kappa$, $\Delta=0$
[25]	UPB + two-photon dissipation	0.38	0.54	$\Omega=0.4\kappa_2$, $\Delta=0$

Single-photon sources based on quantum dots (QDs) in finely tuned microcavities such as micropillars[35] and open cavities[36] have achieved remarkable performance: Ding *et al.*[37] reported an overall system efficiency of 71.2%, a photon indistinguishability of 98.56%, and a multi-photon probability of 2.05%, achieved through optical microcavity optimization and pulse shaping techniques. These advances have propelled QD sources from laboratory demonstrations to practical applications, with key breakthroughs in electrical pumping and on-chip integration. Nevertheless, such performance relies critically on strong coupling, which poses challenges for scalability. Here, we propose an alternative scheme based on UPB combined with two-photon dissipation that exhibits stable photon blockade without requiring strong coupling or fine-tuned cavities. Our system offers abundant tuning dimensions including the driving strength, two-photon loss rate, and detuning, and the synergistic optimization of these parameters enables significant enhancement of single-photon source performance. Analytical calculations indicate that our scheme can achieve a second-order correlation function $g^{(2)}(0)\sim10^{-8}$, representing exceptionally high single-photon purity. While the current QD platform leads in absolute efficiency and indistinguishability, our scheme provides a complementary route particularly suited for superconducting quantum circuit implementations,[38,39] where two-photon dissipation can be engineered using standard nonlinear circuit elements, in contrast to optical platforms, where special nonlinear absorbing media are required.

5. Conclusion

In this work, we propose a scheme to realize UPB in a Kerr nonlinear single-mode cavity by introducing an optical parametric amplification (OPA) and two-photon dissipation. Employing the non-Hermitian Hamiltonian formalism, we obtain the optimal UPB conditions through analytical solution of the Schrödinger equation and validate them through numerical simulation of the master equation with two-photon dissipation. Then we identify photon blockade through the second-order correlation function $g^{(2)}(0)$ and quantify its strength via the mean photon number $\langle n\rangle$. The analytical and numerical solutions exhibit good overall agreement; the minor discrepancy near the minima of $g^{(2)}(0)$ arises from the truncation of the Hilbert space to two-photon states in analytical calculations. Most importantly, we observe that the UPB effect can be enhanced while maintaining high mean photon number by introducing two-photon dissipation. Furthermore, the influences of driving strength, OPA gain, and driving phase on UPB are investigated. Finally, we elucidate the physical mechanism responsible for UPB generation in this system, which explains why the UPB effect can remain stable across a broad range of Kerr nonlinearity strengths. Our proposal offers insights into investigating the PB effect, and it may be applied to generate high-quality single-photon sources.

Appendix A: The optimal UPB condition

When the probability amplitude of the two-photon state $C_2=0$, the optimal condition for UPB in this work is given by

$$2\mathrm{e}^{2\mathrm{i}\phi}\Omega^2-2\mathrm{i}G\Delta-G\kappa=0, \tag{A1}$$

we use Euler's formula

$$\mathrm{e}^{2\mathrm{i}\phi}=\cos2\phi+\mathrm{i}\sin2\phi, \tag{A2}$$

and set the real and imaginary parts of Eq. (13) equal to zero

$$\begin{cases}2\Omega^2\cos2\phi-G\kappa=0,\\ 2\Omega^2\sin2\phi-2\Delta G=0.\end{cases} \tag{A3}$$

Solving the above equations with Mathematica yields the optimal conditions for Eq. (14) in the paper.

References

[1] Kimble H J, Dagenais M and Mandel L 1977 *Phys. Rev. Lett* **39** 691
[2] Eisaman M D, Fan J and Migdall A 2011 *Rev. Sci. Instrum.* **82** 071101
[3] Couteau C, Barz S, Durt T, Gerrits T, Huwer J and Prevedel R 2023 *Nat. Rev. Phys.* **5** 326
[4] Witzel W M, Shabaev A and Hellberg C S 2010 *Phys. Rev. Lett* **105** 137401
[5] Li A, Chen T, Zhou Y H and Wang X B 2016 *Opt. Lett.* **41** 1921
[6] Chunnilall C J, Degiovanni I P and Kück S 2014 *Opt. Eng.* **53** 081910
[7] Kok P, Munro W J and Nemoto K 2007 *Rev. Mod. Phys.* **79** 135
[8] Buckley S, Rivoire K and Vučković J 2012 *Rep. Prog. Phys.* **75** 126503
[9] Shields A J 2007 *Nat. Photonics* **1** 215
[10] Wang H, Gu X, Liu Y X, Miranowicz A and Nori F 2015 *Phys. Rev. A* **92** 033806
[11] Qu Y, Li J and Wu Y 2019 *Phys. Rev. A* **99** 043823
[12] Ren Y, Duan S, Xie W, Shao Y and Duan Z 2021 *Phys. Rev. A* **103** 053710
[13] Shen C P, Li H W, Zhou Y Y, Yang X L, Zeng Y and Wang Y 2026 *Phys. Rev. A* **113** 033701
[14] Werner M J and Imamoglu A 1999 *Phys. Rev. A* **61** 011801(R)
[15] Majumdar A and Gerace D 2013 *Phys. Rev. B* **87** 235319
[16] Shen H Z, Zhou Y H and Yi X X 2014 *Phys. Rev. A* **90** 023849
[17] Hou R, Zhang W, Wang D Y, Su S L, Han X, Wang H F and Zhang S 2023 *Opt. Express* **31** 24939
[18] Liew T C H and Savona V 2010 *Phys. Rev. Lett* **104** 183601
[19] Snijders H J, Frey J A and Norman J 2018 *Phys. Rev. Lett* **121** 043601

[20] Lv G H, Hou R, Zhou Y H, Han X, Wang H F and Zhang A S 2026 *Opt. Express* **34** 421
[21] Ding Z and Zhang Y 2025 *Appl. Phys. Lett* **127** 144002
[22] Luo Y, Zhang X, Xiao Y, Xu J, Li H, Yang Y and Xia X 2025 *Chin. Phys. B* **34** 014203
[23] Zhou Y H, Zhang X Y, Liu T, Wu Q C, Shi Z C, Shen H Z and Yang C P 2022 *Phys. Rev. Appl.* **18** 064009
[24] Feng L J, Ni J and Gong S Q 2024 *Opt. Express* **32** 5117
[25] Zhou Y H, Liu T, Zhang X Y, Wu Q C, Shi Z C and Yang C P 2024 *Phys. Scr.* **99** 095114
[26] Zhang Z Q 2025 *Acta Phys. Sin.* **74** 164205 (in Chinese)
[27] Zhang Z Q 2025 *Optoelectronic. Prog.* **62** 0719001
[28] McNeil K J and Walls D F 1974 *J. Phys. A* **7** 617
[29] Guerra E S, Garraway B M and Knight P L 1997 *Phys. Rev. A* **55** 3842
[30] Plenio M B and Knight P L 1998 *Rev. Mod. Phys.* **70** 101
[31] Li T, Gao Z and Xia K 2021 *Opt. Express* **29** 17613
[32] Noh C 2020 *Sci. Rep.* **10** 16076
[33] Wang C Q, Liu Y L and Wu R B 2017 *Phys. Rev. A* **96** 013818
[34] Zhang H and Duan Z 2023 *Opt. Express* **31** 22580
[35] Ding X, He Y, Duan Z C, Gregersen N, Chen M C, Unsleber S, Maier S, Schneider C, Kamp M 2016 *Phys. Rev. Lett* **116** 020401
[36] Tomm N, Javadi A, Antoniadis N O, Najer D, Korsch A R, Schott R, Valentin S R, Wieck A D, Ludwig A 2021 *Nat. Nanotechnol.* **16** 399
[37] Ding X, Guo Y P, Xu M C, Liu Z, Zou G Y, Zhao J Y, Ge Z X, Zhang Q H, Liu H L, Wang L J 2025 *Nat. Photonics* **19** 387
[38] Felicetti S, Rossatto D Z, Rico E, Solano E and Forn-Díaz P 2018 *Phys. Rev. A* **97** 013851
[39] Gertler J M, Geldern S V, Shirol S, Jiang L and Wang C 2023 *PRX Quantum* **4** 020319